The methylotrophic yeast *Hansenula polymorpha* contains an inducible import pathway for peroxisomal matrix proteins with an N-terminal targeting signal (PTS2 proteins)

(peroxisomes/protein import/amine oxidase/malate dehydrogenase/thiolase)

KLAAS NICO FABER[†], PETER HAIMA[†‡], CHRISTINE GIETL[§], WIM HARDER[†], GEERT AB[¶], AND MARTEN VEENHUIS[†‖]

[†]Laboratory for Electron Microscopy, Biological Centre, University of Groningen, Kerklaan 30, 9751 NN Haren, The Netherlands; [§]Institute of Botany, Technical University of Munich, Arcisstrasse 16, D-80333 Munich, Germany; and [¶]Laboratory of Biochemistry, University of Groningen, Nijenborgh 4, 9747 AG Groningen, The Netherlands

ABSTRACT Two main types of peroxisomal targeting signals have been identified that reside either at the extreme C terminus (PTS1) or the N terminus (PTS2) of the protein. In the methylotrophic yeast *Hansenula polymorpha* the majority of peroxisomal matrix proteins are of the PTS1 type. Thus far, for *H. polymorpha* only amine oxidase (AMO) has been shown to contain a PTS2 type signal. In the present study we expressed *H. polymorpha* AMO under control of the strong endogenous alcohol oxidase promoter. Partial import of AMO into peroxisomes was observed in cells grown in methanol/(NH₄)₂SO₄-containing medium. However, complete import of AMO occurred if the cells were grown under conditions that induce expression of the endogenous AMO gene. Similar results were obtained when the heterologous PTS2 proteins, glyoxysomal malate dehydrogenase from watermelon and thiolase from *Saccharomyces cerevisiae*, were synthesized in *H. polymorpha*. The import of PTS1 proteins, however, was not affected by the growth conditions. These results indicate that the reduced rate of AMO import in (NH₄)₂SO₄-grown cells is not due to competition with PTS1 proteins for the same import pathway. Apparently, AMO is imported via a separate pathway that is induced by amines and functions for PTS2 proteins in general.

In the methylotrophic yeast *Hansenula polymorpha* the development of peroxisomes is induced by a number of unusual carbon and nitrogen sources (1, 2). In particular, during growth on methanol many large peroxisomes develop. These organelles contain the key enzymes alcohol oxidase (AO), dihydroxyacetone synthase (DHAS), and catalase (CAT) of methanol metabolism. Less pronounced induction of the organelles is observed during growth on various organic nitrogen sources—e.g., primary amines, D-amino acids, and purines.

Two different types of peroxisomal targeting signals (PTSs) have been identified that are essential and sufficient to direct newly synthesized precursor proteins to their target organelle. The first PTS identified was the tripeptide SKL, located at the extreme C terminus of firefly luciferase (3, 4). Subsequently, this motive, and degenerate forms of it, were shown to be functional in mammals, insects, plants, and yeasts as well (4, 5). The second PTS type was found in rat thiolase and comprises the first 11 amino acids of the thiolase presequence (6, 7). Comparisons to other microbody proteins revealed a similar sequence in peroxisomal thiolases from yeast (*Saccharomyces cerevisiae, Candida tropicalis,* and *Yarrowia lipolytica*) as well as other matrix proteins that lack a clear PTS1—namely, amine oxidase (AMO) from *H. poly-*

morpha, malate dehydrogenase (MDH) from watermelon, and aldolase from *Trypanosoma brucei*. On the basis of the sequence identities, a general consensus, RL-X₅-H/QL, has been proposed (5). Deletion analysis and site-directed mutagenesis confirmed the presence of an N-terminal targeting signal in *S. cerevisiae* thiolase and watermelon MDH (8, 9). However, also substitutions outside the consensus appear to affect targeting of the protein (8, 10).

PTS1 and PTS2 proteins not only contain different targeting signals but also may use separate import pathways (11). This was concluded from the isolation of various peroxisome-deficient yeast strains (*PER3/PAS8/PAS10*) that are blocked in the import of PTS1 proteins only, while PTS2 proteins—e.g., thiolase—are correctly sorted to peroxisomes (refs. 12–14; M.V., unpublished results). Moreover, a *S. cerevisiae* mutant has been isolated with the opposite phenotype—namely, proper import of PTS1 proteins and cytosolic location of thiolase (14, 15).

In *H. polymorpha,* most of the peroxisomal matrix proteins identified to date contain a PTS1 signal—e.g., AO, DHAS, and CAT (16, 17). However, we have obtained strong indications that peroxisomal AMO, a key enzyme in amine metabolism, contains an N-terminal, PTS2-like signal (RL-X₅-QA). Deletion analysis revealed that essential targeting information is located within the the extreme N-terminal 16 amino acids. Moreover, this sequence can direct a reporter protein, bacterial β-lactamase, to the peroxisomal matrix of *H. polymorpha* (K.N.F., W.H., G.AB, and M.V., unpublished results). To obtain more information on the PTS2 import machinery we have expressed AMO under the control of the endogenous AO promoter (P_AOX), leading to unusually high levels of this protein under methylotrophic growth conditions. In this paper we present evidence that efficient import of the "heterologous" AMO protein as well as other heterologous PTS2 proteins is dependent on induction of a specific component(s) of the import machinery.

MATERIALS AND METHODS

Yeast Strains and Growth Conditions. Transformants of *H. polymorpha* A16 (18), carrying the AMO gene under the control of the P_AOX (*H. polymorpha* GF15 and GF16; see below), were grown in C source-limited chemostat cultures on mineral medium containing a mixture of glucose (0.25%,

Abbreviations: AO, alcohol oxidase; DHAS, dihydroxyacetone synthase; CAT, catalase; AMO, amine oxidase; PTS, peroxisomal targeting signal; MDH, malate dehydrogenase; gMDH, glyoxysomal MDH; WT, wild type; D, dilution rate.
[‡]Present address: Nichols Institute Diagnostics, Nieuwe Weg 172, 6603 BT Wijchen, The Netherlands.
[‖]To whom reprint requests should be addressed.

wt/vol) and methanol (0.25%, vol/vol) as carbon source and $(NH_4)_2SO_4$ (0.25%, wt/vol) as nitrogen source or glucose (0.25%, wt/vol) as sole carbon source and choline (0.20%, wt/vol) as nitrogen source (19). Fresh medium was added at a dilution rate (D) of 0.085 per hr. Transformed strains, carrying the heterologous gene coding for glyoxysomal MDH (gMDH) from watermelon (strain GF58) or thiolase from *S. cerevisiae* (strain GF91) under control of the P_{AOX}, were grown in shaker flasks in mineral medium (20) on methanol (0.5%, vol/vol) as carbon source and $(NH_4)_2SO_4$ (0.25%, wt/vol) or methylamine (0.20%, wt/vol) as nitrogen source.

Plasmid Constructions. pHIPX1 (Fig. 1*A*) was constructed from the following DNA fragments (numbers indicate nucleotide position on pHIPX1) [(*) sticky ends filled in using Klenow enzyme; (**) sticky ends removed by mung bean nuclease]: (1–40) *Hin*dIII–*Cla* I(*) fragment from pTZ19R containing part of the polylinker (21). The *Cla* I site originates from digestion with *Bam*HI(*) and religation. (41–340) *Xho* I(*)–*Hin*dIII(*) fragment containing the *H. polymorpha* AMO

FIG. 1.   (*A*) Physical map of the expression plasmids pHIPX1 and pHIPX2. Insertion of the *H. polymorpha* amine oxidase gene (*AMO*) yields plasmids pGF71 and pGF72. (*B*) Schematic representation of the chromosomal *AOX* locus in *H. polymorpha* A16 [wild type (WT)] and the transformed strains GF15 and GF16 resulting from integration of the plasmids pGF71 or pGF72 in the genome. (*C*) Southern analysis of *H. polymorpha* A16 (lane 1), GF15 (lane 2), and GF16 (lane 3). Total DNA was digested with *Eco*RI, and the banding pattern is a result of hybridization with a 2.3-kb *Bam*HI–*Hin*dIII DNA fragment from pHIPX2 containing P_{AOX}. B, *Bam*HI; E, *Eco*RI; H, *Hin*dIII; Sc, *Sac* I; Sp, *Sph* I.

terminator region (T_{AMO}) (22). (341–619/620–2840) contains the *S. cerevisiae* phosphoglycerate kinase terminator region (T_{PGK}) and the *LEU2* gene from *S. cerevisiae* and is identical to (442–820/821–3041) from pHIPX4 (9). (2840–4260) *Bgl* II–*Bam*HI(*) *H. polymorpha* genomic DNA fragment present downstream of the *AOX* gene containing the major part of the open reading frame encoding anthranilate synthase component II (23). The *Bam*HI site was created at the position of a *Sac* I site by digestion with *Sac* I(**) and ligation to a *Bam*HI(*) site. (4260–6660) *Cla* I(*)–*Bam*HI fragment from pHP7 (24) from which the part of the multiple cloning site [*Hin*dIII(**)–*Sal* I(**) and religation] was deleted. (6660–8700) *Bam*HI–*Hin*dIII *H. polymorpha AOX* promoter region (P_{AOX}) (25). The *Hin*dIII site is created as described for pHIPX4 (9). pHIPX2 (Fig. 1*A*) was constructed analogous to pHIPX1 with some minor differences (stated below), without including the 1.4-kb *Bgl* II–*Bam*HI *TRP2* fragment. Coordinates: (1–45) *Hin*dIII–*Sma* I, polylinker pTZ19R; (45–360) *Sma* I–*Hin*dIII(*), T_{AMO}; (360–640) *Bgl* II(*)–*Hin*dIII(*), T_{PGK}; (640–2860) *Hin*dIII(*)–*Bgl* III(*), *LEU2*; (2860–5280) *Cla* I–*Bam*HI, pHP7; (5280–7320) *Bam*HI–*Hin*dIII, P_{AOX}.

A 2.2-kb *Hin*dIII–*Sac* I fragment encoding the *AMO* gene from *H. polymorpha* (22) was inserted in these expression vectors digested with the same restriction enzymes, resulting in plasmids pGF71 and pGF72, respectively.

A cDNA fragment encoding glyoxysomal malate dehydrogenase was cloned as a 1.3-kb *Not* I(*)–*Sal* I (−8/+1280) fragment (26) into *H. polymorpha* expression vector pHIPX4 (9) digested with *Hin*dIII(*)–*Sal* I resulting in pGF192. A 1.3-kb *Dde* I(partial)(*)–*Bam*HI(*) (−36/+1290) DNA fragment from pRE157 (gift from W.-H. Kunau, Bochum, Germany) containing the thiolase gene from *S. cerevisiae* was inserted into pHIPX4 digested with *Hin*dIII(*)–*Sma* I, resulting in pGF224.

Molecular Genetic Manipulation and Yeast Transformation. Standard genetic procedures were essentially as described (27). *Escherichia coli* DH1 (*supE44 hsdR17 recA1 endA1 gyrA96 thi-1 relA1*) was used for plasmid amplification and grown on LB medium. *H. polymorpha* A16 was transformed by electroporation (28). Prior to transformation the expression vectors pGF71 and pGF72 were linearized by *Bam*HI or *Sph* I digestion, respectively, forcing integration of the plasmid DNA at the homologous locus on the genome (24). This results in either the addition of the plasmid-encoded expression unit in the *AOX* promoter locus (pGF72) or the replacement of the chromosomal *AOX* gene by the linearized plasmid (pGF71) (Fig. 1*B*). Transformants that have the plasmid integrated in the genome (integrants) were selected by growth of transformants for ≈40 generations on nonselective medium. Correct integration was confirmed by Southern blot analysis (29) using the ECL direct nucleic acid labeling and detection system from Amersham. Strain GF15 contains plasmid pGF71 integrated in the genome and is therefore AOX^- (methanol utilizing minus, Mut⁻). Strain GF16 contains plasmid pGF72 in the genome (AOX^+). Expression plasmids containing pre-gMDH (pGF192) and thiolase (pGF224) were used to transform *H. polymorpha* A16 and were maintained as circular autonomous replicating plasmids in the host. Transformants were checked by retransformation of *E. coli* with total yeast DNA.

Biochemical Methods. Cell extracts were prepared as described (30). Protein concentrations were determined with the Bio-Rad protein assay kit using bovine serum albumin as a standard. Enzyme activities of AO (31) and AMO (32) were assayed as described and expressed as μmol of substrate consumed per min per mg of protein. The cell extracts were analyzed by SDS/PAGE (33). Gels were stained with Coomassie brilliant blue R-250 or subjected to immunoblotting (Protoblot immunoblot system; Promega) using polyclonal antibodies raised against AMO (α-AMO). Transfer of
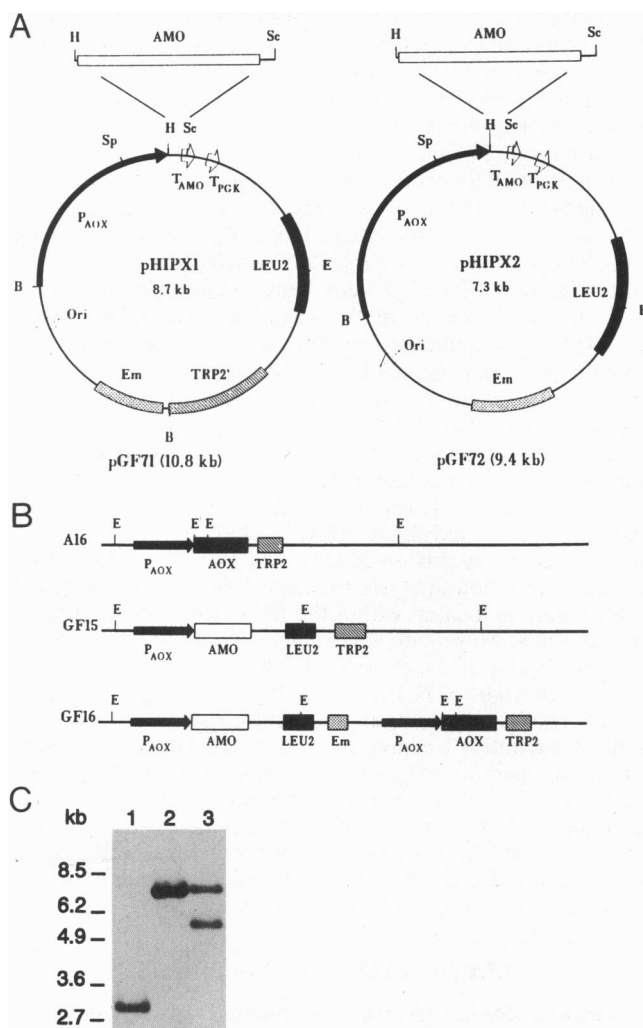
Cell Biology: Faber *et al.*

Proc. Natl. Acad. Sci. USA 91 (1994)   12987

proteins onto nitrocellulose after SDS/PAGE was performed according to ref. 34 using a semidry blotter (Ancos, Højby, Denmark).

Electron Microscopy. Intact cells and spheroplasts were prepared for electron microscopy as described (35). Immunocytochemistry was performed on ultrathin sections of Lowicryl K₄M-embedded cells by the protein A/gold method (36), using polyclonal antibodies raised against AMO (α-AMO), gMDH from watermelon (α-gMDH), or thiolase from *S. cerevisiae* (α-thiolase). Cytochemical staining experiments for determining the subcellular localization of AMO activity were performed by the Ce^{3+} method (37).

RESULTS

Transformation and Strain Selection. *H. polymorpha* was transformed with two different plasmids, pGF71 and pGF72. Following the isolation of integrants, two strains, GF15 and GF16, were selected by Southern blot analysis (Fig. 1C). Each of these strains contained one additional copy of the *AMO* gene under the control of the P_{AOX} present in the genomic *AOX* locus. Whereas the endogenous *AMO* gene had been retained in both strains, the *AOX* gene had been deleted from the genome in strain GF15. The strains were subsequently grown under various conditions to study synthesis and peroxisomal import of AMO.

P_{AOX}-Controlled AMO Synthesis. In glucose/(NH₄)₂SO₄-grown cells of strains GF15 and GF16, no AMO protein was detected. However, after shifting these cells to batch cultures containing a mixture of glycerol/methanol in the presence of (NH₄)₂SO₄ as nitrogen source, AMO activity was detected within 2 hr of incubation. As expected, WT cells contained no AMO protein under these conditions, indicating that the presence of AMO in the transformants must be due to P_{AOX}-driven synthesis.

To obtain maximal expression levels of (P_{AOX}-driven) heterologous AMO, the two transformants were grown in carbon-limited chemostat cultures (D = 0.085 per hr) on glucose/methanol in the presence of (NH₄)₂SO₄ as sole nitrogen source. In WT cells these conditions result in massive induction of AO constituting up to 30% of total cellular protein (38). Analysis of cell-free extracts of the chemostat-grown GF16 cells revealed the presence of high levels of AMO protein (Table 1; Fig. 2), exceeding the amount of 10% of total cellular protein. Cells of strain GF15 grown under the same conditions also synthesized AMO, although to a 4-fold lower level than observed in cells of strain GF16. The reason for this difference is unclear but may very well reflect differences in specific cultivation conditions—e.g., dissolved oxygen concentrations (39). As expected AO activity was present to WT levels in strain GF16, whereas it was invariably absent in strain GF15 (Table 1).

Cell Morphology and Subcellular Location of AMO Protein. Cells of strain GF16 contained many large peroxisomes with a largely crystalline matrix due to the crystallization of AO protein (1, 2). Peroxisomes in cells of strain GF15 were reduced in size and lacked crystalloids. Localization of

Table 1. Enzyme activities (AO/AMO) in cell-free extracts prepared from cells of strains GF15 and GF16 grown in continuous cultures (D = 0.085 per hr) on glucose/methanol/(NH₄)₂SO₄ or glucose/choline

Growth conditions	GF15		GF16	
	AO	AMO	AO	AMO
Glucose/methanol/(NH₄)₂SO₄	0	0.10	4.50	0.40
Glucose/choline	0	0.43	3.20	0.43

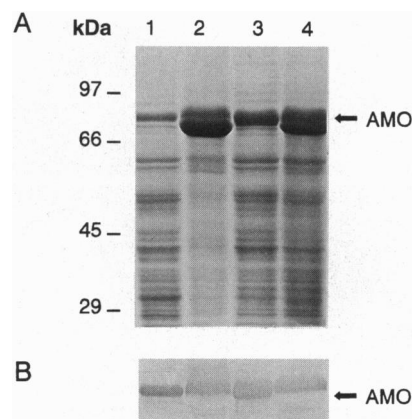Enzyme activities are expressed as μmol of substrate consumed per min per mg of protein.

FIG. 2. SDS/PAGE analysis of soluble proteins from strains GF15 (lanes 1 and 3) and GF16 (lanes 2 and 4). Cells were grown in chemostat cultures on glucose/methanol/(NH₄)₂SO₄ (lanes 1 and 2) or glucose/choline (lanes 3 and 4). (*A*) Coomassie brilliant blue-stained gel. (*B*) AMO protein band identified by immunoblotting. The dominant band below the AMO band in lanes 2 and 4 represents AO and DHAS (both ±75 kDa). Expression levels of AMO in these strains were quantified by comparison of the intensities of the AMO protein bands in Coomassie brilliant blue-stained SDS/polyacrylamide gels with standard amounts of purified AMO.

heterologous expressed AMO in glucose/methanol/(NH₄)₂SO₄-grown cells was determined by cytochemistry and immunocytochemistry (Figs. 3 and 4). These studies indicated that, independent of the genotype, AMO was partly localized in peroxisomes and in the cytosol. Import of typical PTS1 matrix proteins was not impaired as was indicated by the labeling patterns of AO (Fig. 5A), DHAS, and CAT (data not shown), which were solely peroxisomal. These results suggest that the partial import of AMO did not result from saturation of the import capacity of individual peroxisomes but may reflect a specific impairment in the import of AMO.
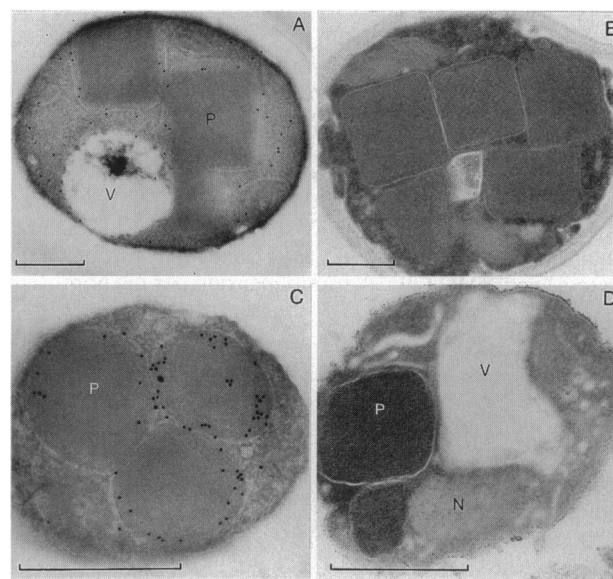

FIG. 3. AMO location in strain GF16. AMO protein (by immunocytochemistry) and activity (by cytochemistry) were determined in cells grown under AMO-repressing [glucose/methanol/(NH₄)₂SO₄] or inducing (glucose/choline) conditions. In cells grown in the presence of (NH₄)₂SO₄, cytosolic and peroxisomal AMO was found (*A*, anti-AMO, protein A/gold; *B*, Ce^{3+} activity staining). In amine-induced cells (glucose/choline), AMO protein (*C*) and activity (*D*) were confined to the peroxisomal matrix. N, nucleus; P, peroxisomes; V, vacuole. (Bars = 0.5 μm.)
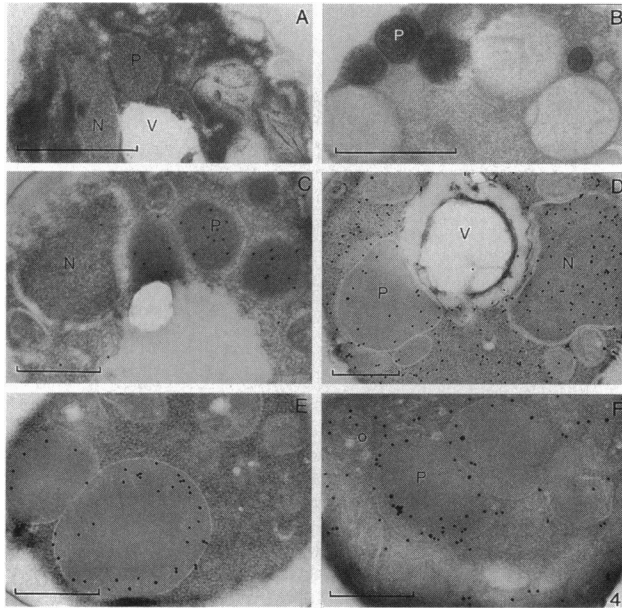
FIG. 4.   (*A–C*) AMO location studies in strain GF15. AMO protein (by immunocytochemistry) and activity (by cytochemistry) were determined in cells grown under AMO-repressing [glucose/methanol/(NH₄)₂SO₄] or inducing (glucose/choline) conditions. In cells grown in the presence of (NH₄)₂SO₄, cytosolic and peroxisomal AMO was found (*A*, Ce^{3+} activity staining). In amine-induced cells (glucose/choline), AMO activity (*B*, Ce^{3+} activity staining) and protein (*C*, anti-AMO, protein A/gold) were confined to the peroxisomal matrix. (*D–F*) Location of heterologous PTS2 proteins when expressed in *H. polymorpha* under AMO-repressing and AMO-inducing conditions determined by immunocytochemistry (anti-gMDH, protein A/gold; anti-thiolase, protein A/gold). In (NH₄)₂SO₄-grown cells, watermelon gMDH in strain GF58 (*D*) and *S. cerevisiae* thiolase in strain GF93 (*F*) were found in peroxisomes, the cytosol, and the nucleus, whereas in methylamine-grown cells, these heterologous PTS2 proteins were found solely in the peroxisome (*E*, strain GF58, gMDH). N, nucleus; P, peroxisomes; V, vacuole. (Bars = 0.5 μm.)

The fact that in WT cells grown under the above conditions synthesis of AMO is fully repressed may suggest that a specific component essential for efficient import of AMO is lacking.

Efficient Import of Heterologous AMO Was Dependent on Specific Growth Conditions. WT cells of *H. polymorpha* grown in a chemostat on glucose/choline at a low D accumulate optimal levels of AO (3–4 μmol per min per mg of protein) and AMO (20–30 mμmol per min per mg of protein),
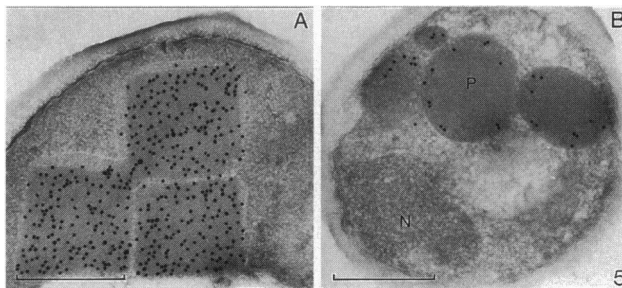

FIG. 5.   AO and thiolase location in GF16 and GF58, respectively. AO protein was determined immunocytochemically in cells of strain GF16, grown under AMO-repressing conditions [glucose/methanol/(NH₄)₂SO₄] and found to be confined to the peroxisomal matrix (*A*; anti-A, protein A/gold). A similar location was found for bakers' yeast thiolase in cells of strain GF58, grown under AMO-inducing conditions (*B*; anti-thiolase, protein A/gold). N, nucleus; P, peroxisome. (Bars = 0.5 μm.)

which are completely imported into peroxisomes (19, 40). Under these conditions the synthesis of heterologous AMO in the transformants was also enhanced as is apparent from the AMO activity of at least 400 mμmol per min per mg of protein (Table 1), which is 20-fold higher than in WT. Again, AO was normally induced to WT levels (3.5 μmol per min per mg of protein) in GF16 but was lacking in GF15. As is evident from immuno- and enzyme cytochemistry (Figs. 3 and 4), AMO was solely present in peroxisomes, irrespective of whether expressed in the AO⁻ (GF15) or AO⁺ (GF16) environment.

This suggests that efficient import of AMO is dependent on a component that, together with endogenous AMO, is induced by the amine substrate.

The Inducible Import Pathway Is Specific for PTS2 Proteins. To determine whether the inducible import pathway is specifically involved in sorting of PTS2 proteins in general, we studied the import of two heterologous PTS2 proteins in *H. polymorpha*—namely, *S. cerevisiae* thiolase and watermelon gMDH. Previously we showed that watermelon gMDH was correctly sorted to peroxisomes in *H. polymorpha* (41). In the present study, enhanced expression levels of both heterologous genes were obtained by specific adaptations of the growth conditions of the cells. In particular, precultivation under stringent selective conditions (e.g., in the absence of yeast extract) led to enhanced protein levels, probably as a result of a higher plasmid copy number. We found that import of both heterologous proteins followed the same patterns, as described above for AMO. Thus, at high expression levels, only part of the *S. cerevisiae* thiolase and watermelon gMDH protein was detected inside peroxisomes, whereas the remaining part accumulated in the cytosol (and nucleus) (Fig. 4 *D* and *F*). On the basis of the identical staining patterns, obtained in immunocytochemical experiments, efficient and complete import of watermelon gMDH (Fig. 4*E*) and bakers' yeast thiolase (Fig. 5*B*), however, occurred in cells grown in the presence of methylamine as sole N source.

DISCUSSION

In this paper we present evidence for the existance of an inducible import pathway for peroxisomal matrix proteins with a PTS2-type targeting signal, which functions separate from the import pathway for PTS1 proteins.

The presence of different import machineries for peroxisomal matrix proteins was predicted earlier from the analysis of various peroxisome-deficient yeast strains that are impaired in the import of matrix proteins containing either a PTS1 or a PTS2 signal (12–14). The import machinery for PTS2 proteins in *H. polymorpha* appears to be inducible. This can be deduced from our data on *H. polymorpha* transformants, either expressing the homologous *AMO* gene or the heterologous watermelon gMDH and *S. cerevisiae* thiolase genes under the control of the *H. polymorpha AOX* promoter (P_{AOX}). Efficient (and complete) import of these PTS2 proteins solely occurred when the cells were grown under conditions in which the synthesis of endogenous AMO was induced. Earlier experiments with various yeast strains have shown that the total protein storage capacity of the organelles is not fully used in normal WT cells. This is indicated by the findings that the organelles are able to import artificially overexpressed matrix giving rise to a considerable increase in organellar size (16, 42, 43). Only at very high expression levels did the import capacity become saturated, resulting in the accumulation of the additional amounts of protein in the cytosol.

Two findings argue against the possibility that such conditions are met in our present experiments. (*i*) All heterologous synthesized matrix proteins (AMO, watermelon gMDH, or *S. cerevisiae* thiolase) were fully imported in amine-grown

Cell Biology: Faber *et al.*

Proc. Natl. Acad. Sci. USA 91 (1994)   12989

cells. (*ii*) In the AO$^+$ (GF16) and AO$^-$ (GF15), identical distribution patterns of heterologous AMO were observed. Furthermore, the fact that solely PTS2 proteins (but not PTS1 proteins) remain partly cytosolic in (NH$_4$)$_2$SO$_4$-grown cells, excludes a possible competition of precursor proteins for one general import pathway. Therefore, our results led us to conclude that the import rate rather than the import storage capacity is limiting in (NH$_4$)$_2$SO$_4$-grown cells, a restriction that is abolished during growth of cells in the presence of amines as sole N source.

It is not yet clear which mechanism accounts for the partial import of PTS2 proteins in (NH$_4$)$_2$SO$_4$-grown *H. polymorpha* cells. In *S. cerevisiae PAS10* and *Pichia pastoris PAS8* deletion mutants, which lack the putative SKL receptor, solely PTS2 proteins were imported into the peroxisomal matrix (12, 13). A similar result was obtained in the phenotypically analogous *H. polymorpha PER3* deletion strain (M.V., unpublished). The opposite situation is found in the *S. cerevisiae PAS7* mutant, which excludes thiolase from the peroxisomes but not PTS1 proteins (14). These results suggest that the separate PTS1 and PTS2 import machineries are fully specific and cannot complement for each other's functions.

The PTS1 import machinery is functional in fully repressed glucose-grown *H. polymorpha* cells as is indicated by the efficient import and assembly of AO under these conditions (42). In line with this we assume that the low-rate import of PTS2 proteins in (NH$_4$)$_2$SO$_4$-grown *H. polymorpha* is due to the presence of the specific PTS2 import pathway, however at basal levels. In fact, both import machineries appear to be inducible and are in particular present at enhanced levels in cells in which the synthesis of peroxisomes is induced by specific growth substrates. Our data on *H. polymorpha PER3*, together with the findings by Subramani and co-workers (12) on *P. pastoris PAS8*, indicate that the corresponding gene products (Per3p and Pas8p, respectively) are induced severalfold ($\approx$8- to 10-fold) in methanol-grown cells, compared to the levels found on glucose. However, during growth of *H. polymorpha* on glucose the basal level of components involved in import of PTS1 proteins is sufficient to account for efficient import of heterologous expressed PTS1 protein. Although the (protein) nature of the components involved in the import of PTS2 proteins in *H. polymorpha* are still unknown it is tempting to suggest that either a cytosolic component or a specific membranous component(s) is the limiting factor(s) in (NH$_4$)$_2$SO$_4$-grown cells. Identification of the components of the PTS2 import machinery in *H. polymorpha* warrants investigation.

1. Veenhuis, M. & Harder, W. (1991) in *The Yeasts*, eds. Rose, A. H. & Harrison, J. S. (Academic, London), 2nd Ed., Vol. 4, pp. 601–653.
2. Veenhuis, M. (1992) *Cell Biochem. Funct.* **10**, 175–184.
3. Gould, S. J., Keller, G.-A. & Subramani, S. (1987) *J. Cell Biol.* **105**, 897–905.
4. Subramani, S. (1993) *Annu. Rev. Cell Biol.* **9**, 445–478.
5. de Hoop, M. J. & AB, G. (1992) *Biochem. J.* **286**, 657–669.
6. Swinkels, B. W., Gould, S. J., Bodnar, A. G., Rachubinski, R. A. & Subramani, S. (1991) *EMBO J.* **10**, 3255–3262.
7. Osumi, T., Tsukamoto, T., Hata, S., Yokota, S., Miura, S.,
8. Fujiki, Y., Hijikata, M., Miyazawa, S. & Hashimoto, T. (1991) *Biochem. Biophys. Res. Commun.* **181**, 947–954.
8. Glover, J. R., Andrews, D. W., Subramani, S. & Rachubinski, R. A. (1994) *J. Biol. Chem.* **269**, 7558–7563.
9. Gietl, C., Faber, K. N., Van der Klei, I. J. & Veenhuis, M. (1994) *Proc. Natl. Acad. Sci. USA* **91**, 3151–3155.
10. Tsukamoto, T., Hata, S., Yokata, S., Miura, S., Fujiki, Y., Hijikata, M., Miyazawa, S., Hashimoto, T. & Osumi, T. (1994) *J. Biol. Chem.* **269**, 6001–6010.
11. Zhang, J. W., Luckey, C. & Lazarow, P. B. (1993) *Mol. Biol. Cell* **4**, 1351–1359.
12. McCollum, D., Monosov, E. & Subramani, S. (1993) *J. Cell Biol.* **121**, 761–774.
13. Van der Leij, I., Franse, M. M., Elgersma, Y., Distel, B. & Tabak, H. F. (1993) *Proc. Natl. Acad. Sci. USA* **90**, 11782–11786.
14. Erdmann, R. & Kunau, W.-H. (1992) *Cell Biochem. Funct.* **10**, 167–174.
15. Van der Leij, I., Van der Berg, M., Boot, R., Franse, M. M., Distel, B. & Tabak, H. F. (1992) *J. Cell Biol.* **119**, 153–162.
16. Hansen, H., Didion, T., Thiemann, A., Veenhuis, M. & Roggenkamp, R. (1992) *Mol. Gen. Genet.* **235**, 269–278.
17. Didion, T. & Roggenkamp, R. (1992) *FEBS Lett.* **303**, 113–116.
18. Veale, R. A., Giusseppin, M. L. F., Van Eijk, H. M. J., Sudbery, P. E. & Verrips, C. T. (1992) *Yeast* **8**, 361–372.
19. Van der Klei, I. J., Sulter, G. J., Harder, W. & Veenhuis, M. (1991) *Yeast* **7**, 15–24.
20. Veenhuis, M., Keizer, I. & Harder, W. (1979) *Arch. Microbiol.* **120**, 167–175.
21. Mead, D. A., Szczesna-Skorupa, E. & Kemper, B. (1986) *Protein Eng.* **1**, 67–74.
22. Bruinenberg, P. G., Evers, M. E., Waterham, H. R., Kuipers, J., Arnberg, A. C. & AB, G. (1989) *Biochim. Biophys. Acta* **1008**, 157–167.
23. Reid, G. A. (1988) *Nucleic Acids Res.* **16**, 6236.
24. Faber, K. N., Swaving, G. J., Faber, F., AB, G., Harder, W., Veenhuis, M. & Haima, P. (1992) *J. Gen. Microbiol.* **138**, 2405–2416.
25. Ledeboer, A. M., Edens, L., Maat, J., Visser, C., Bos, J. W. & Verrips, C. T. (1985) *Nucleic Acids Res.* **13**, 3063–3082.
26. Gietl, C. (1990) *Proc. Natl. Acad. Sci. USA* **87**, 5773–5777.
27. Sambrook, J., Fritsch, E. F. & Maniatis, T. (1989) *Molecular Cloning: A Laboratory Manual* (Cold Spring Harbor Lab. Press, Plainview, NY), 2nd Ed.
28. Faber, K. N., Haima, P., Harder, W., Veenhuis, M. & AB, G. (1994) *Curr. Genet.* **25**, 305–310.
29. Southern, E. (1975) *J. Mol. Biol.* **98**, 503–517.
30. Waterham, H. R., Keizer-Gunnink, I., Goodman, J. M., Harder, W. & Veenhuis, M. (1992) *J. Bacteriol.* **174**, 4057–4063.
31. Verduyn, C., Van Dijken, J. P. & Scheffers, W. A. (1984) *J. Microbiol. Methods* **2**, 15–25.
32. Zwart, K. B., Veenhuis, M., Van Dijken, J. P. & Harder, W. (1980) *Arch. Microbiol.* **126**, 117–126.
33. Laemmli, U. K. (1970) *Nature (London)* **227**, 680–685.
34. Kyhse-Andersen, J. (1984) *J. Biochem. Biophys. Methods* **10**, 203–209.
35. Keizer-Gunnink, I., Roggenkamp, R., Harder, W. & Veenhuis, M. (1992) *FEMS Microbiol. Lett.* **93**, 7–12.
36. Slot, J. W. & Geuze, H. J. (1984) in *Immunolabeling for Electronmicroscopy*, eds. Polak, J. M. & Varndell, I. M. (Elsevier, New York), pp. 129–142.
37. Veenhuis, M., van Dijken, J. P. & Harder, W. (1976) *Arch. Microbiol.* **111**, 123–135.
38. Veenhuis, M., Van Dijken, J. P. & Harder, W. (1983) *Adv. Microbiol. Physiol.* **24**, 1–82.
39. Van Dijken, J. P., Otto, R. & Harder, W. (1976) *Arch. Microbiol.* **111**, 137–144.
40. Zwart, K. B., Veenhuis, M., Plat, G. & Harder, W. (1983) *Arch. Microbiol.* **136**, 28–38.
41. Van der Klei, I. J., Faber, K. N., Keizer-Gunnink, I., Gietl, C., Harder, W. & Veenhuis, M. (1993) *FEBS Lett.* **334**, 128–132.
42. Distel, B., Van der Leij, I., Veenhuis, M. & Tabak, H. F. (1988) *J. Cell Biol.* **107**, 1669–1675.
43. Roggenkamp, R., Didion, T. & Kowallik, K. V. (1989) *Mol. Cell. Biol.* **9**, 988–994.